Journal of Science and Technology in Transportation Volume 1 Issue 1, 2020
ISSN: 2710-XXXX DOI: 10.XXXX/jstit.202002_1(1).0001

Influence of Carrier Phase Shifted SPWM on Output Voltage of Multilevel Converter for Rail Transit

Liujian Zhang[1], Xun Wang[1,*]

[1.] Southwest Jiaotong University, Chengdu, Sichuan, China

[*] Corresponding Email, wangxun0323@126.com

Abstract

The converter is one of the core components of traction drive system, which determines the traction force and speed of train operation. Carrier phase shifted SPWM modulation method could ensure that each power unit outputs the same voltage and frequency at any modulation ratio or fundamental frequency, and maintain the same switching frequency, so it has been widely used in converter. In this work, the influence of carrier phase shifted SPWM on output voltage of converter was analysed. The results show that number of series N is an even number, the control effect of phase shift angle π/N is obviously better than that of phase shift angle $2\pi/N$, N is an odd number, the two methods have the same control effect. The number of phase voltage and line voltage levels decreases with the decrease of modulation ratio m, and the THD of line voltage and phase voltage increases with the decrease of m. Therefore, when designing multilevel converter, a large modulation ratio should be selected.

Keywords

Carrier phase shifted SPWM; Converter; Output voltage

1 Introduction

Traction drive system as shown in Figure 1 is the power source of rail transit vehicles, which determines the running speed of rail transit vehicles. The traction drive system [1-3] is composed of pantograph, traction transformer, pulse rectifier, traction inverter and traction motor, etc. The pantograph transmits AC 25 kV single-phase power frequency AC of the catenary to the traction transformer. The single-phase AC after voltage reduction by the transformer is supplied to the pulse rectifier, which converts the single-phase output AC into DC. Output DC to traction inverter through intermediate DC circuit, the traction inverter outputs three-phase AC with controllable voltage, current and frequency to the three-phase asynchronous traction motor [4-6]. The torque and speed output by the shaft end of the traction motor are

ISSN: 2710-XXXX DOI: 10.XXXX/jstit.202002_1(1).0001

transmitted to the wheel set through gear transmission and converted into wheel traction force and linear speed.

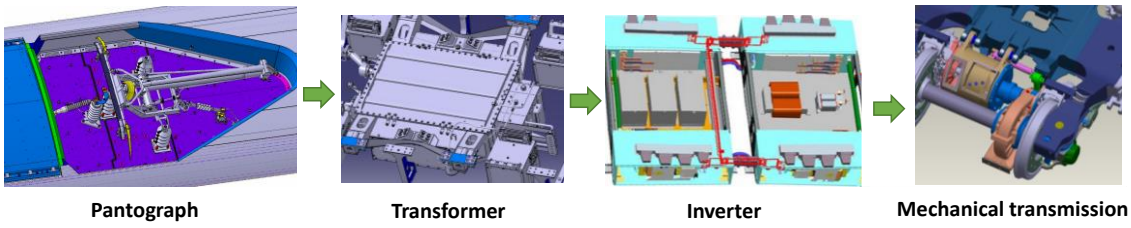

Figure 1 Main components of traction drive system for rail transit.

In the traction drive system [7-9], the AC with adjustable amplitude and frequency output by the frequency converter is supplied to the traction motor, so as to control the traction force and running speed of the train [10, 11]. The better the working effect of the frequency converter, the less the torque harmonic content of the motor output would be, which is conducive to the safety, stability and comfort of rail transit vehicles [12][13]. High voltage inverter is applied because of its high input power factor, many output phase voltage levels, good output voltage waveform and small harmonic component. Its control methods and modulation algorithms are diverse.

At present, the widely used frequency converter control methods [14, 15] are vector control and direct torque control. Vector control decouples stator current into excitation component and torque component through coordinate transformation. These two components are independent of each other. The purpose of controlling magnetic field and torque can be realized by controlling them separately, so that asynchronous motor [16-18] control has the same excellent performance as DC motor control. Different from the decoupling method used in vector control, direct torque control directly controls the torque of the motor by rapidly changing the slip speed of the motor magnetic field to the rotor, so as to obtain the high-performance state of the torque.

The common modulation algorithms of frequency converter [19, 20] mainly include multi carrier PWM modulation algorithm and space vector SVPWM modulation algorithm. Multi carrier PWM modulation algorithm is the most commonly used method of high-voltage inverter. Generally, multiple carriers are compared with modulation wave. According to the different arrangement of carriers, the methods of generating PWM wave can be divided into carrier stacking method and carrier phase-shifting SPWM method [21, 22]. Space voltage vector SVPWM takes the ideal flux circle of the stator of the three-phase symmetrical motor when the three-phase symmetrical sine wave voltage is supplied as the reference standard, and makes appropriate switching with different switching modes of the three-phase inverter, so as to form PWM wave, and track its accurate flux circle with the formed actual flux vector. In this work, the influence of frequency converter carrier phase shifted SPWM modulation algorithm on output voltage was analysed.

2 Frequency converter carrier phase shifted SPWM modulation algorithm

Each phase of the modular multi-level high-voltage converter is composed of N identical power units in series. The working principle of each power unit as shown in Figure 2 is as follows: after the three-phase AC is rectified by the diode uncontrolled

ISSN: 2710-XXXX DOI: 10.XXXX/jstit.202002_1(1).0001

full bridge rectifier circuit, the DC bus voltage is formed by the filter capacitor, and the output side is the H-bridge single-phase inverter circuit composed of four IGBT modules, The output voltage of variable voltage and frequency conversion is obtained by PWM modulation. Because the rectifier part of the power unit is a diode uncontrolled rectifier structure, it cannot realize energy feedback, so it cannot operate in four quadrants.

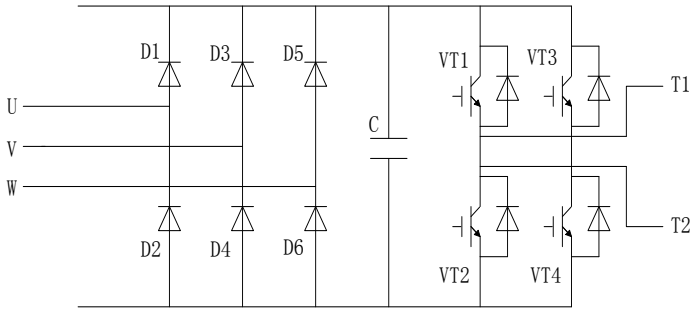

Figure 2 Power unit circuit structure of modular multi-level high-voltage converter.

The carrier phase shifted SPWM modulation method can ensure that each power unit outputs the same voltage and frequency and maintains the same switching frequency at any modulation ratio or fundamental frequency. Moreover, the output voltage PWM waveform of each power unit is basically the same, and there is no imbalance of output power between power units. Under the same carrier frequency, the output voltage frequency of carrier horizontal phase shifted SPWM is N times of carrier frequency. The advantages of carrier phase-shifting SPWM make it the standard control method of modular multi-level high-voltage converter. There are two control methods of carrier phase-shifting SPWM: unipolar PWM control and bipolar PWM control.

Unipolar PWM modulation algorithm, its triangular carrier changes only in one polarity range in half a cycle. As shown in Figure 3, in the positive half cycle of the modulation wave Ur, the carrier U_C is a positive triangular wave, in the negative half cycle of the modulation wave Ur, the carrier U_C is a negative triangular wave, and the intersection of U_C and Ur is the time to control the power device on and off.

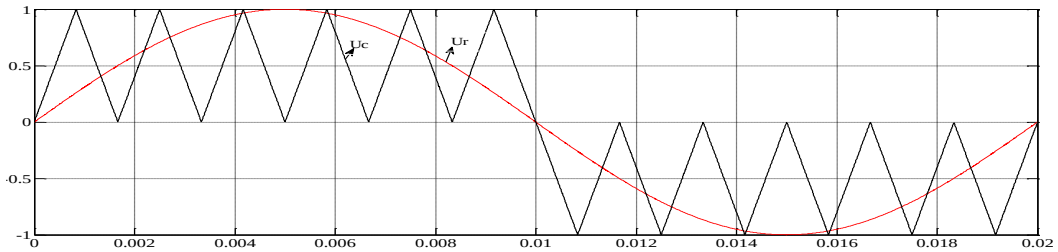

Figure 3 Schematic diagram of unipolar PWM modulation.

In bipolar in-phase PWM modulation, the left bridge arm modulation wave phase is consistent with the output voltage phase, while the right bridge arm modulation wave is opposite. By Fourier decomposition of the output voltage of the left bridge arm of a single power unit, the output voltage relationship of the left bridge arm of the power unit could be obtained:

ISSN: 2710-XXXX DOI: 10.XXXX/jstit.202002_1(1).0001

$$U_{a11}=\frac{ME}{2}\cos(\omega t)+\frac{2E}{\pi}\sum_{m=1}^{\infty}\sum_{n=-\infty}^{\infty}\frac{1}{m}\left\{\sin[(m+n)\frac{\pi}{2}]J_{\mathrm{n}}(m\frac{\pi}{2}M)\cos(m\omega_{\mathrm{c}}t+n\omega t)\right\}$$

Because the phase difference of the modulation wave between the left and right bridge arms of the same power unit is 180 °, the expression of the output voltage of a phase single power unit is:

$$U_{\mathrm{a1}}=U_{\mathrm{a11}}-U_{\mathrm{a12}}=ME\cos(\omega t)+\frac{4E}{\pi}\sum_{m=1}^{\infty}\sum_{n=-\infty}^{\infty}\frac{1}{m}\cdot\{\cos[(m+n+1)\pi]J_{\mathrm{2n\text{-}1}}m\pi M$$
$$\cdot\cos[2m\omega_{\mathrm{c}}t+(2n-1)\omega t]\}$$

When N power units are connected in series, the expression of output phase voltage is:

$$U_{\mathrm{a}}=\sum_{i=1}^{N}U_{\mathrm{ai}}=NME\cos(\omega t)+\frac{4E}{\pi}\sum_{m=1}^{\infty}\sum_{n=-\infty}^{\infty}\frac{1}{m}\cdot\{\cos[(m+n+1)\pi]J_{\mathrm{2n\text{-}1}}m\pi M$$
$$\cdot\sum_{i=1}^{N}\cos[2m(\omega_{\mathrm{c}}t+\frac{i\pi-\pi}{N})+(2n-1)\omega t]\Big\}$$

Here, E—Bus voltage of power unit, M—Modulation ratio, ω—The frequency of the output fundamental voltage, ω_{c}—The frequency of the triangular carrier.

In carrier phase shifted out of phase PWM modulation, two modulation waves of power unit are provided by two phases respectively. And different from in-phase modulation, the left and right bridge arm modulation waves of its power unit change, that is, the phase of the left bridge arm modulation wave is consistent with the output voltage, while the phase angle of the right bridge arm modulation wave lags 120 °. The output voltage of single power unit and phase A shall could meet the following requirements:

$$\begin{cases}U_{a1}=\dfrac{\sqrt{3}}{2}ME\sin(\omega t+\pi/6)\\ U_{\mathrm{AN}}=\sum_{n=1}^{5}U_{\mathrm{an}}ME\sin(\omega t+\pi/6)\end{cases}$$

3 Analysis of factors affecting output voltage of carrier phase shifted SPWM

3.1 Effect of phase shift angle on output voltage

There are two phase-shifting modes in carrier phase-shifting SPWM modulation, one is phase-shifting π/N angle, the other is phase-shifting 2π/N angle. The selection of phase shift angle will affect the level and harmonic content of output voltage.

ISSN: 2710-XXXX DOI: 10.XXXX/jstit.202002_1(1).0001

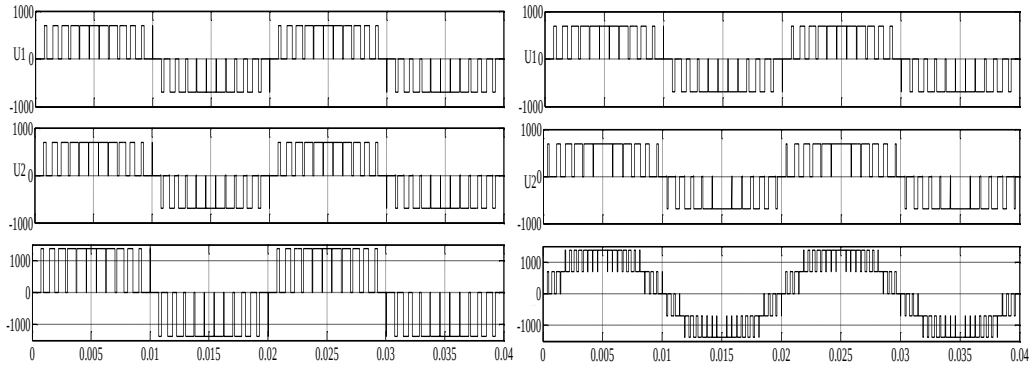

(a) The phase shift angle is π (b) The phase shift angle is π/2

Figure 4 Output voltage waveform (*N*= 2) at two phase shifting modes, (a) shift angle π, and (b) shift angle π/2.

As shown in Figure 4, the phase voltage waveforms corresponding to different phase shifting modes when two power units are connected in series. As can be seen from the figure, when the phase shift angle is π, the output voltage is three-level; When the phase shift angle is π/2, the output voltage is five levels, and the performance is superior to the former.

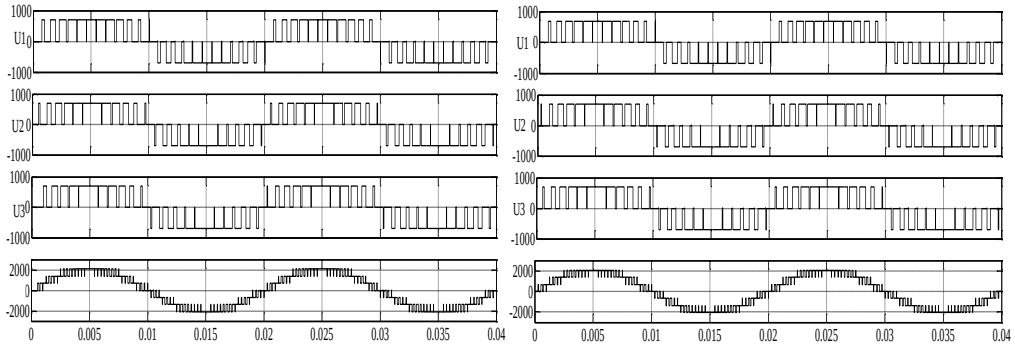

(a) The phase shift angle is 2π/3 (b) The phase shift angle is π/3

Figure 5 Output voltage waveform (*N*= 3) at two phase shifting modes, (a) shift angle 2π/3, and (b) shift angle π/3.

The phase voltage waveforms corresponding to different phase shifting modes are shown in Figure 5 when three power units are connected in series. It can be seen from the figure that the control effects of the two are the same.

Further analyzing and summarizing the two cases of N=4 and N=5. The results are shown in Table 1.

Table 1 Comparative analysis of influence of phase shift angle on output voltage.

Number of series, N	The phase shift angle is π / N		The phase shift angle is 2π / N	
	Number of output phase voltage levels	THD (%)	Number of output phase voltage levels	THD (%)
2	5	26.96	3	51.93
3	7	18.24	7	18.13

ISSN: 2710-XXXX DOI: 10.XXXX/jstit.202002_1(1).0001

4	9	13.77	5	26.81
5	11	11.07	11	11.04

It can be seen from Table 1 that as the number of power units in series increases, the level number of output phase voltage also increases, and the total voltage distortion rate decreases. Moreover, when N is an even number, the control effect of phase shift angle π/N is obviously better than that of phase shift angle 2π/N. When N is an odd number, the two methods have the same control effect.

3.2 Effect of modulation ratio m on output voltage

The relationship between the number of output levels of phase voltage of high-voltage inverter and the number of power units in series *N* satisfies 2n+1, but this is only true in the linear region and not in the nonlinear region.

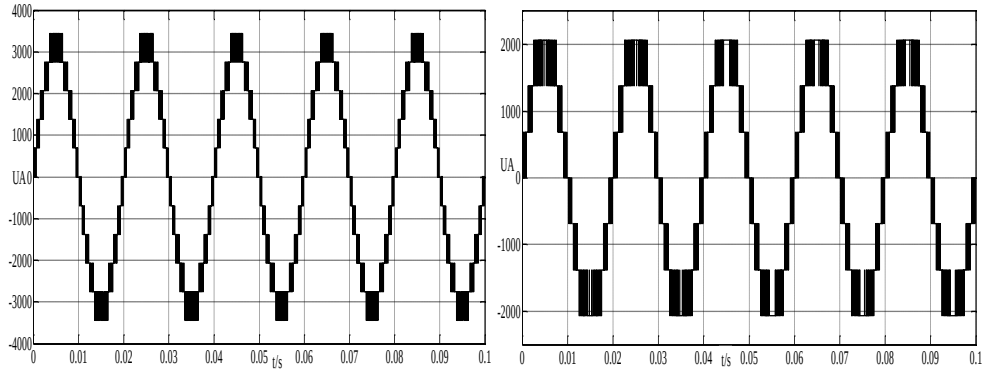

(a) m=0.9 (b) m=0.6

Figure 6 Waveform of output phase voltage at different amplitude ratio.

As shown in Figure 6 and Figure 7, The levels of phase voltage and line voltage increase with the increase of modulation ratio, and the sinusoidal degree of waveform becomes better and better.

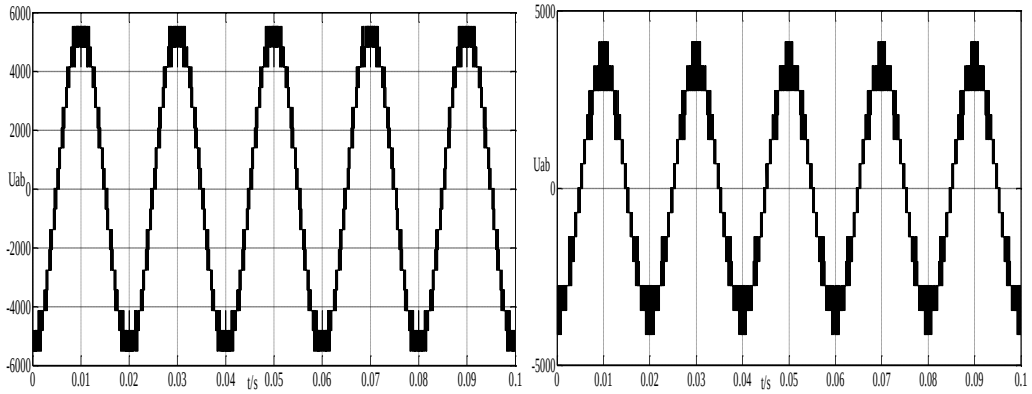

(a) m=0.9 (b) m=0.6

Figure 7 Waveform of output line voltage at different amplitude ratio.

When the value of m changes, the changes of the level number of phase voltage and line voltage and the changes of harmonics are shown in Table 2.

ISSN: 2710-XXXX DOI: 10.XXXX/jstit.202002_1(1).0001

Table 2 Comparison of effects of different modulation ratios on output voltage.

Modulation ratio, m	Phase voltage		Line voltage	
	Level number	THD (%)	Level number	THD (%)
1	11	10.97	21	8.38
0.95	11	12.46	21	9.69
0.9	11	13.15	17	10.99
0.8	9	13.58	17	12.16
0.7	9	16.79	15	13.59
0.6	7	17.75	13	14.76
0.5	7	23.64	13	19.25
0.4	5	26.48	9	25.39
0.3	5	39.89	9	28.52
0.2	3	52.07	5	39.13

It can be seen from Table 2 that the number of phase voltage and line voltage levels decreases with the decrease of m, and the THD of line voltage and phase voltage increases with the decrease of m. Therefore, when designing high-voltage frequency converter, a large modulation ratio should be selected. Generally, the value of m should be greater than 0.8.

4 Conclusions

Carrier phase shifted SPWM modulation algorithm can improve the equivalent switching frequency and reduce the harmonic content of output voltage. Its output current has good sinusoidal degree. It is very suitable for the modulation mode of modular multi-level high-voltage converter. The simulation results show that the number of phase voltage and line voltage levels decreases with the decrease of m, and the THD of line voltage and phase voltage increases with the decrease of m. As the number of power units in series increases, the level number of output phase voltage also increases, and the total voltage distortion rate decreases. Moreover, when N is an even number, the control effect of phase shift angle π/N is obviously better than that of phase shift angle $2\pi/N$. When N is an odd number, the two methods have the same control effect.

Acknowledgements

Southwest Jiaotong University Graduate Scholarship was greatly acknowledged, and thanks also gave to the support of editors and the platform.

References

1. Anh A. T. T. and Phuong V. H., *Braking energy recuperation for electric traction drive in urban rail transit network based on control super-capacitor energy storage system.* Journal of Electrical Systems, 2018. **14**(3): 99-114.

ISSN: 2710-XXXX DOI: 10.XXXX/jstit.202002_1(1).0001

2. Chen Z. W., Li X. M., Yang C., Peng T., Yang C. H., Karimi H. R., *A data-driven ground fault detection and isolation method for main circuit in railway electrical traction system.* Isa Transactions, 2019. **87**: 264-271.
3. Dolecek R., Cerny O., Novak J., and Bartlomiejczyk M., *Interference in Power system for traction drive with PMSM.* Przeglad Elektrotechniczny, 2012. **88**(9A): 204-207.
4. Niu G. and Liu S. Y., *Demagnetization monitoring and life extending control for permanent magnet-driven traction systems.* Mechanical Systems and Signal Processing, 2018. **103**: 264-279.
5. Pahner U., Hameyer K., and Belmans R., *A parallel implementation of a parametric optimization environment - Numerical optimization of an inductor for traction drive systems.* Ieee Transactions on Energy Conversion, 1999. **14**(4): 1329-1334.
6. Reyhart D. R. and Anwar S., *Optimal control of an On-Demand All-Wheel Drive system (ODAWD) for vehicle traction enhancement.* International Journal of Vehicle Design, 2011. **56**(1-4): 270-298.
7. Dybkowski M., Orlowska-Kowalska T., and Tarchala G., *Sensorless Traction Drive System with Sliding Mode and MRAS(CC) Estimators using Direct Torque Control.* Automatika, 2013. **54**(3): 329-336.
8. Dybkowski M., Tarchala G., Orlowska-Kowalska T., and Kazmierkowski M. P., *Analysis of the sensorless traction drive system with sliding mode observer.* Przeglad Elektrotechniczny, 2012. **88**(6): 216-220.
9. Fukui R., Okabe T., Nakao M., and Honda Y., *Highly efficient traction drive system with a normal force controller using a piezoelectric actuator.* Advances in Mechanical Engineering, 2017. **9**(10).
10. Stana G., Brazis V., and Apse-Apsitis P., *Simulation of Induction Traction Drive with Supercapacitor Energy Storage System Test Bench.* Electrical Control and Communication Engineering, 2015. **9**(1): 14-22.
11. Taniguchi S., Yasui K., Yuki K., Nakazawa Y., and Onda S., *A Restart Control Method for Position Sensorless PMSM Drive Systems Without Potential Transformer for Railway Vehicle Traction.* Electrical Engineering in Japan, 2015. **193**(3): 44-53.
12. Gou Bin, Ge Xinglai, Wang Shunliang, Feng Xiaoyun, Kuo James B., and Habetler Thomas G., *An Open-Switch Fault Diagnosis Method for Single-Phase PWM Rectifier Using a Model-Based Approach in High-Speed Railway Electrical Traction Drive System.* IEEE Transactions on Power Electronics, 2016. **31**(5): 3816-3826.
13. Konowrocki R., *Modelling of dynamic aspects of operation in railway vehicle traction drive system including the electromechanical coupling.* Scientific Journal of Silesian University of Technology-Series Transport, 2019. **105**: 101-111.
14. Drabek P., Peroutka Z., Pittermann M., and Cedl M., *New Configuration of Traction Converter With Medium-Frequency Transformer Using Matrix Converters.* Ieee Transactions on Industrial Electronics, 2011. **58**(11): 5041-5048.
15. He X., Williams B. W., Green T. C., and Finney S. J., *A novel unified passive lossless turn-on and turn-off snubber for high-frequency power converter applications.* International Journal of Electronics, 1996. **81**(3): 337-359.
16. Wang H. M., Ge X. L., and Liu Y. C., *An Active Damping Stabilization Scheme for the Suppression of the DC-Link Oscillation in Metro Traction*

ISSN: 2710-XXXX **DOI: 10.XXXX/jstit.202002_1(1).0001**

Drive System. Ieee Transactions on Industry Applications, 2018. **54**(5): 5113-5123.

17. Yang C. H., Yang C., Peng T., Yang X. Y., and Gui W. H., *A Fault-Injection Strategy for Traction Drive Control Systems.* Ieee Transactions on Industrial Electronics, 2017. **64**(7): 5719-5727.
18. Yousfi D., Belkouch S., Ouahman A. A., Grenier D., Dehez B., and Richard E., *Design of PM Motor Drive Course and DSP Based Robot Traction System Laboratory.* Journal of Power Electronics, 2010. **10**(6): 647-659.
19. Lin B. R., *Series-Connected High Frequency Converters in a DC Microgrid System for DC Light Rail Transit.* Energies, 2018. **11**(2).
20. Morimoto K., Fathy K., Ogiwara H., Lee H. W., and Nakaoka M., *DC rail side series switch and parallel capacitor snubber-assisted edge resonant soft-switching PWM DC-DC converter with high-frequency transformer link.* Journal of Power Electronics, 2007. **7**(3): 181-190.
21. Sayed K. F., Nakaoka M., Morimoto K., and Kwon S. K., *New high-frequency linked half-bridge soft-switching PWM DC-DC converter with input DC rail side active edge resonant snubbers.* Iet Power Electronics, 2010. **3**(5): 774-783.
22. Wickramasinghe T., Kularatna N., and Steyn-Ross A., *Reduced-switch SCALDO: an extra low-frequency DC-DC converter technique for VRM applications.* Iet Power Electronics, 2017. **10**(15): 2180-2189.